buckling slopes are given by the dashed lines. The combined effects of increasing γ and pressure increase the direction of initial postbuckling from an extreme slope almost doubling back on the original prebuckling displacement curve to a slope of roughly half that of the prebuckled slope. The wide variation in initial postbuckling slopes shown in Fig. 8a can be expected to decrease as θ decreases. The extreme slopes at low pressure move counterclockwise with decreasing θ, while the limiting slope at high pressure changes very slightly. For example, the $\theta = 0.7$ case for $\gamma = 0$ closely approximates that given in Fig. 8c.

6. Concluding Remarks

The effects of internal pressure and edge stiffener torsional rigidity on buckling and initial postbuckling behavior have been presented. The study is conducted within the context of the Kármán-Donnell equations and Koiter's initial postbuckling theory. It has been shown that even moderate values of torsional rigidity significantly reduce the panel imperfection sensitivity. An internal pressure can also aid in making the panel more insensitive to small geometric imperfections. In addition, the values of the panel flatness parameter for which the analysis is valid is increased by including the torsional rigidity of the stiffener. In the limit where torsional rigidity and internal pressure are zero, the present results reduce exactly to the original results of Koiter.

References

[1] Koiter, W. T., "Buckling and Postbuckling Behavior of a Cylindrical Panel Under Axial Compression," Rept. S.476, 1956, National Aeronautical Research Institute, Amsterdam.

[2] Budiansky, B., "Post-Buckling Behavior of Cylinders in Torsion," *IUTAM Symposium, Copenhagen, 1967, Theory of Thin Shells*, edited by F. I. Niordson, Springer-Verlag, New York, 1969.

[3] Budiansky, B. and Amazigo, J. C., "Initial Postbuckling Behavior of Cylindrical Shells Under External Pressure," *Journal of Mathematics and Physics*, Vol. 47, No. 3, Sept. 1968, pp. 223–235.

[4] Budiansky, B., unpublished lecture notes, 1969, Harvard Univ., Cambridge, Mass.

[5] Hutchinson, J. W., "Buckling and Initial Postbuckling Behavior of Oval Cylindrical Shells Under Axial Compression," *Transactions of the ASME: Ser. E*, Vol. 35, No. 1, March 1968, pp. 66–72.

SEPTEMBER 1971 AIAA JOURNAL VOL. 9, NO. 9

Finite-Element Analysis of Large Elastic-Plastic Transient Deformations of Simple Structures

RICHARD W. H. WU* AND EMMETT A. WITMER†
Massachusetts Institute of Technology, Cambridge, Mass.

The assumed-displacement finite-element method which is based upon the Principle of Virtual Work is extended to analyze the large-deflection transient responses of simple structures including elastic-plastic, strain-hardening, and strain-rate material behavior. The resulting equations of motion are solved by a direct timewise numerical integration scheme using the central-difference procedure. Numerical examples are carried out and compared with both finite-difference predictions and experimental results for an impulsively loaded beam and an impulsively loaded ring.

Introduction

THE conventional closed form analysis/prediction of structural transient responses which involve large deformations and nonlinear material behavior is rendered practically impossible by the complexities arising from these two sources of nonlinearities. In practice, therefore, one is usually forced to employ numerical prediction methods.

Numerical methods of structural analysis may be described conveniently in two categories. In the first category is the "finite-element method" which is most systematically based upon variational principles[1]; the solid continuum is idealized as an assemblage of a finite number of regions which are connected at a finite number of nodes along interelement (or interregion) boundaries, with the geometry and the material properties of the continuum being faithfully retained in the idealized structural assembly. The second category, "the numerical solution of the governing algebraic and/or differential equations," is based upon mathematically approximating and solving the differential equations by either finite differences[2–4] or by numerical integration.[5–7] In the past several years, the finite-element method has undergone intensive development and has proved to be a very effective and powerful method for analyzing certain classes of problems such as small-deflection, linear-elastic, static, and dynamic response behavior.[8–11] For predicting large-deflection, elastic-plastic transient response of structures, the finite-difference approach[3,4,12–14] has been much more extensively developed than the finite-element method; corresponding developments of the finite-element method to treat this class of problems would be valuable. A contribution to this area is the subject of this study.

Among the finite-element analyses for large-deflection linear-elastic behavior including both static and transient responses are the developments reported in Ref. 15 for shells of revolution. In Ref. 15, large deflection terms are treated as equivalent force terms which are derived from the pertinent energy expressions in the variational formulation employed; for those special terms, a linear rather than a cubic displacement field for the normal displacement is used in order to

Received September 21, 1970, revision received January 4, 1971.

* Graduate Student in the Aeroelastic and Structures Research Laboratory (MIT-ASRL) of the Department of Aeronautics and Astronautics.

† Professor of Aeronautics and Astronautics.

avoid numerical difficulties, and represents a plausible approximation. Iterative and extrapolative procedures for handling those terms in solving the equations of motion are investigated. The inclusion of nonlinear (elastic-plastic) material behavior as well as large deflections in the finite-element approach is described and predictions are given, for example, in Refs. 16 and 17 for static problems, and in Ref. 18 the finite-element formulation of the equilibrium equation is given and an incremental stiffness equation is derived; however, no transient response analysis is reported in Ref. 18. Reference 16 utilizes the initial strain concept for including plastic behavior while Refs. 17 and 18 employ the tangent modulus approach; in all of these cases a linearized incremental formulation results.

Recently Salus, Ip, and Vanderlinden[19] have described the formulation and application of a finite-element approach for predicting the large-deflection elastic-plastic transient response behavior of beam-type structures. The resulting predictions, for several examples reported, are in good agreement with finite-difference predictions and with experimental results. This formulation is of the assumed displacement type but is not based upon variational principles; lumping of masses and external loads is used. Emphasizing the plastic part of the behavior, only linear displacement fields are introduced for all of the displacements, and transverse shear deformation is included. While elastic, perfectly plastic material behavior is taken into account, the effect of transverse shear deformation on yielding and flow appears to be accounted for only in an indirect fashion.

In the present study the assumed-displacement finite-element approach, which is based upon the Principle of Virtual Work (displacements) and D'Alembert's Principle, is applied to analyze the large-displacement, elastic-plastic, strain-hardening, transient, Kirchhoff-type responses of general curved beams. In this formulation, the Lagrangian description is used. The assumed-displacement field includes the rigid-body modes exactly. The mass and the externally applied loads are included in a variationally consistent fashion. The resulting equations of motion are solved numerically in a time-wise step-by-step manner using the central-difference procedure.

Formulation of the Governing Equations

For a continuum in equilibrium (static or dynamic, and with arbitrary deformation conditions consistent with the prescribed displacement boundary conditions), the Principle of Virtual Work states that

$$\delta U - \delta W = 0 \tag{1}$$

where

$$\delta U = \iiint_{V_0} S^{ij}\delta\gamma_{ij}dV = \text{variation of the internal energy} \tag{2}\ddagger$$

$$\delta W = \iiint_{V_0} \rho_0 B^i \delta u_i dV + \iint_A T^i \delta u_i dA = \text{variation of the}$$

of the body forces B^i work (inertia, gravity, magnetic, etc.) per unit mass of the body and of the externally applied surface tractions T^i. (3)

In these equations S^{ij} is the Kirchhoff stress tensor (based upon a unit area of the undeformed body), γ_{ij} is the strain tensor, u_j represents the displacement components, ρ_0 represents the mass per unit volume of the undeformed body, and only displacement variations (δ) are permitted. All pertinent quantities are described with respect to a set of initial (intrinsic, Lagrangian) Cartesian coordinates ξ^i.

Subdividing the continuum into n finite elements or regions, Eq. (1) may be written by summing the contributions from each of the finite elements as follows:

$$\sum_{n=1}^{n} (\delta U_n - \delta W_n) = 0 \tag{4}$$

where

$$\delta U_n = \iiint_{V_n} S^{ij}\delta\gamma_{ij}dV \tag{5}$$

$$\delta W_n = \iiint_{V_n} \rho_0 B^i \delta u_i dV + \iint_{A_{n(\text{out})}} T^i \delta u_i dA + \iint_{A_{n(\text{in})}} T^i \delta u_i dA \tag{6}$$

In Eqs. (4–6), V_n is the volume of element n, $A_{n(\text{in})}$ is the surface area of element n which is shared with mating elements, and $A_{n(\text{out})}$ is the remaining surface area of element n. Both V_n and A_n are referred to the undeformed state.

The strains γ_{ij} may be expressed in terms of the displacements by

$$\begin{aligned}\gamma_{ij} &= \tfrac{1}{2}[u_{i,j} + u_{j,i} + u_{a,i}u^a{}_{,j}] \\ &= \gamma_{ij}{}^L + \gamma_{ij}{}^{NL}\end{aligned} \tag{7}$$

where

$$\gamma_{ij}{}^L = \tfrac{1}{2}[u_{i,j} + u_{j,i}] = \text{linear part} \tag{8}$$

$$\gamma_{ij}{}^{NL} = \tfrac{1}{2}[u_{a,i}u^a{}_{,j}] = \text{nonlinear part} \tag{9}$$

Therefore, if one chooses for each element an assumed displacement field of the form:

$$u_i = [N_i]\{q\} \tag{10}$$

where the $\{q\}$ represent conveniently chosen generalized nodal displacements of the finite element, it follows that

$$\delta u_i = [N_i]\{\delta q\} \tag{11}$$

Hence,

$$\delta\gamma_{ij} = [D_{ij}]\{\delta q\} + [q]\{D_{ai}\}[D_j{}^a]\{\delta q\} \tag{12}$$

where

$$\begin{aligned}[D_{ij}] &= \tfrac{1}{2}([N_{i,j}] + [N_{j,i}]) \\ [D_{ai}] &= [N_{a,i}] \\ [D_j{}^a] &= [N^a{}_{,j}]\end{aligned} \tag{12a}$$

Employing Eqs. (11) and (12) and setting $B^i \equiv -\ddot{u}^i + f^i$, Eq. (4) becomes, in matrix form:

$$\sum_{n=1}^{n} \left(\iiint_{V_n} [\delta q]\{D_{ij}\}S^{ij}dV + \iiint_{V_n} [\delta q]\{D_{ai}\}[D_j{}^a]S^{ij}\{q\}dV + \iiint_{V_n} [\delta q][N]^T\rho_0[N]\{\ddot{q}\}dV - \iiint_{V_n} [\delta q][N]^T\rho_0\{f\}dV - \iint_{A_{n(\text{out})}} [\delta q][N]^T\{T\}dA - \iint_{A_{n(\text{in})}} [\delta q][N]^T\{T\}dA\right) = 0 \tag{13}$$

Before performing the indicated summation over all of the finite elements, it is useful to transform all of the element generalized displacements $\{q\}$ to those for a global reference frame $\{q^*\}$ by

$$\{q\} = [J]\{q^*\} \tag{14}$$

Applying Eq. (14) to Eq. (13), one obtains:

$$\sum_{n=1}^{n} [\delta q^*]([m]\{\ddot{q}^*\} + \{p\} + [h]\{q^*\} - \{Q\} - \{Q_{\text{in}}\}) = 0 \tag{15}$$

where

$$[m] = [J]^T \iiint_{V_n} [N]^T\rho_0[N]dV[J] \tag{16}$$

$$[p] = [J]^T \iiint_{V_n} \{D_{ij}\}S^{ij}dV \tag{17}$$

$$[h] = [J]^T \iiint_{V_n} \{D_{ai}\}[D_j{}^a]S^{ij}dV[J] \tag{18}$$

$$\{Q\} = [J]^T\left(\iiint_{V_n} \rho_0[N]^T\{f\}dV + \iint_{A_{n(\text{out})}} [N]^T\{T\}dA\right) \tag{19}$$

$$\{Q_{\text{in}}\} = [J]^T \iint_{A_{n(\text{in})}} [N]^T\{T\}dA \tag{20}$$

‡ The customary tensor indicial and summation conventions are used. Latin minuscules range over the values 1, 2, and 3.

Performing the indicated summation and noting that terms involving the areas $A_{n(\text{in})}$ cancel out identically, one obtains:

$$[\delta q^*]([M^*]\{\ddot{q}^*\} + \{P\} + [H]\{q^*\} - \{F\}) = 0 \quad (21)$$

Since the δq^* are independent and arbitrary, the following equations of dynamic equilibrium result from Eq. (21):

$$[M^*]\{\ddot{q}^*\} + \{P\} + [H]\{q^*\} = \{F\} \quad (22)$$

Given a set of initial conditions $\{q^*\}$, $\{\dot{q}^*\}$, and $\{F\}$ at $t = 0$, Eqs. (22) may be solved in a step-by-step timewise fashion by using, for example, the central-difference scheme. Further aspects of the solution process are noted later.

It is important to note that in the conventional assumed-displacement finite-element method, quadratic and cubic terms in the displacement variables would appear in the dynamic equation of equilibrium in the form[15]:

$$[M^*]\{\ddot{q}^*\} + [K^*]\{q^*\} = \{F\} + \{R(q^{*2},q^{*3})\} \quad (22a)$$

In the present study, it has been found that, for a given time-wise numerical integration scheme, the formulation denoted by Eq. (22) is well behaved while the formulation expressed by Eq. (22a) is badly behaved (unstable) unless an extremely small time increment is used; therefore Eq. (22) is employed in the present analysis and represents the central contribution of this study.

In connection with Eq. (22), it should be noted that the quantities $[M^*]$ and $\{F\}$ are exactly the same as found in the conventional assumed displacement formulation for small-displacement, linear-elastic behavior as represented by Eq. (22a). The $\{P\}$ in Eq. (22) replaces the usual stiffness terms $[K^*]\{q^*\}$ for small displacements but here also reflect some plastic behavior contributions; the terms $[H]\{q^*\}$ are new and arise because of both large deflections and plastic behavior.

Alternatively, if desired, this formulation could be (and has been) developed in terms of deformation rates etc., by using the less common Principle of Virtual Velocities.

Finally, Eq. (1) can be utilized, if desired, to show that any point in the continuum must satisfy the following equilibrium equations:

$$[S^{im}(\delta_m{}^i + u^i{}_{,m})]_{,j} + \rho_0 f^i = \rho_0 \ddot{u}^i \quad (23)$$

where $\delta_m{}^i$ is the Kronecker delta and $i = 1$, 2, and 3. On the boundary where the surface traction $\bar{T}^i$ is prescribed (denoted by the bar)

$$[S^{im}(\delta_m{}^i + u^i{}_{,m})]_0 n_j = \bar{T}^i \quad (24)$$

where ${}_0n_j$ is the component of the unit outward vector normal to the undeformed surface. Also, on portions of the boundary whereon the displacements $\bar{u}_i$ are prescribed,

$$u_i = \bar{u}_i \quad (25)$$

It should be noted that this formulation pertains to any type of loaded body. In the remainder of this discussion, however, its application is demonstrated only for simple curved and straight beamlike structures which undergo planar (two-dimensional) deformations; in the structural finite-element context, such configurations are termed one-dimensional.

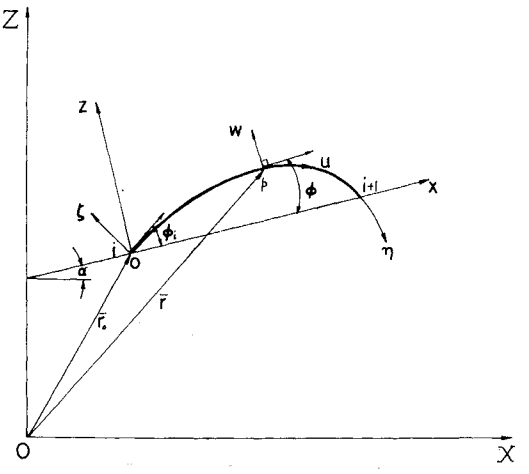

Fig. 1 Nomenclature for geometry, coordinates, and displacements for a curved-beam finite element.

Formulation for a General Curved Beam

Geometry

The discrete element to be considered is a general curved beam as shown in Fig. 1. The slope, ϕ, of the element is assumed to be a second-order polynomial in the curvilinear coordinate, η, as follows:

$$\phi(\eta) = b_0 + b_1\eta + b_2\eta^2 \quad (26)$$

The constants b_0, b_1, and b_2 may be determined from the known geometry of the curved beam element by requiring the slopes of the idealized beam element and the actual beam element to have the same slopes at the nodes and that the ends i and $i + 1$ lie on $z = 0$.

Displacement Field

Employing the Bernoulli-Euler hypothesis, the displacement field $\tilde{u},\tilde{w}$ of the beam may be specified by the middle-plane displacements u and w, and the rotation ψ, as follows:

$$\begin{aligned} \tilde{u}(\zeta,\eta) &= u(\eta) - \zeta\psi(\eta) \\ \tilde{w}(\zeta,\eta) &= w(\eta) \end{aligned} \quad (27)$$

where

$$\psi(\eta) = \frac{\partial w}{\partial \eta} + u\frac{\partial \phi}{\partial \eta} \quad (27a)$$

Considering the beam element in space, if it is subjected to small amplitude rigid-body translations v_x and v_z, and rotation Ω_y with respect to the local reference coordinate system (x,y,z), the rigid-body displacement of any point $p(X,Z)$ is given by

$$\begin{Bmatrix} u \\ w \end{Bmatrix}_{\text{rigid body}} = \begin{bmatrix} \cos\phi & \sin\phi & (Z - Z_0)\cos(\phi + \alpha) - (X - X_0)\sin(\phi + \alpha) \\ -\sin\phi & \cos\phi & -(Z - Z_0)\sin(\phi + \alpha) - (X - X_0)\cos(\phi + \alpha) \end{bmatrix} \begin{Bmatrix} v_x \\ v_z \\ \Omega_y \end{Bmatrix} \quad (28)$$

where X_0 and Z_0 represent the global planar coordinates of the origin of the (x,y,z) coordinate system.

To account for the strain-inducing modes and the rigid-body modes, the assumed displacement field[20] takes the form

$$\begin{Bmatrix} u \\ w \\ \psi \end{Bmatrix} = \begin{bmatrix} \cos\phi & \sin\phi & (Z - Z_0)\cos(\phi + \alpha) - (X - X_0)\sin(\phi + \alpha) & \eta & 0 & 0 \\ -\sin\phi & \cos\phi & -(Z - Z_0)\sin(\phi + \alpha) - (X - X_0)\cos(\phi + \alpha) & 0 & \eta^2 & \eta^3 \\ 0 & 0 & 1 & \eta\dfrac{\partial\phi}{\partial\eta} & 2\eta & 3\eta^2 \end{bmatrix} \begin{Bmatrix} a_1 \\ a_2 \\ a_3 \\ a_4 \\ a_5 \\ a_6 \end{Bmatrix} \quad (29)$$

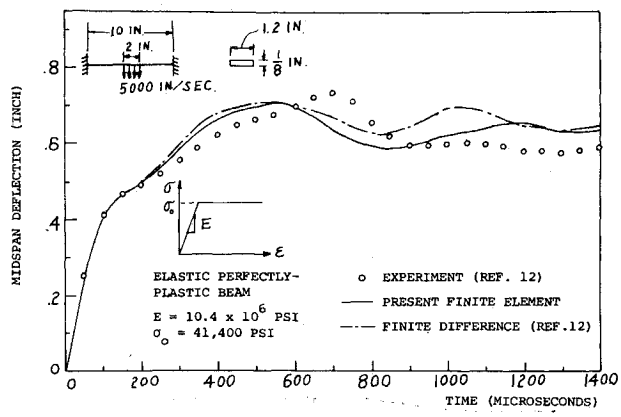

Fig. 2 Midspan deflection response for explosively-loaded clamped 6061-T6 beam.

where $a_1, a_2 \ldots a_6$ are constants which will be expressed in terms of the six selected generalized displacements of the element. In more compact matrix form, Eq. (29) becomes

$$\{\mathbf{u}\} = [S]\{\mathbf{a}\} \tag{30}$$

The generalized displacements $\{q\}$ chosen to characterize the deformation state of this element are selected such that there are three degrees of freedom u, w, and ψ at each node of the element:

$$\{q\} \equiv [u_i\ w_i\ \psi_i\ u_{i+1}\ w_{i+1}\ \psi_{i+1}]^T = [A]\{\mathbf{a}\} \tag{31}$$

If a straight beam is considered, the corresponding quantities can be obtained by letting $\phi = 0$ and $\partial\phi/\partial\eta = 0$.

Strain-Displacement Relations

Under the Bernoulli-Euler hypothesis the only nonvanishing (uniaxial) corresponding stress component and strain component are σ and ϵ, respectively, and the nonlinear strain-displacement relation may be expressed as:

$$\epsilon = \epsilon_0 + \zeta \mathrm{K} \tag{32}$$

where

$$\begin{aligned}\epsilon_0 &= \partial u/\partial\eta - w\partial\phi/\partial\eta + \tfrac{1}{2}[\partial w/\partial\eta + u(\partial\phi/\partial\eta)]^2 \\ &\equiv [B_1]\{\mathbf{u}\} + \tfrac{1}{2}[\mathbf{u}]\{B_2\}[B_2]\{\mathbf{u}\} \\ \mathrm{K} &= -(\partial/\partial\eta)[\partial w/\partial\eta + u(\partial\phi/\partial\eta)] \equiv [B_3]\{\mathbf{u}\}\end{aligned} \tag{33}$$

Combining Eqs. (30–33), one obtains

$$\{\mathbf{u}\} = [N]\{q\} \tag{34}$$

and

$$\begin{aligned}\epsilon_0 &= [D_1]\{q\} + \tfrac{1}{2}[q]\{D_2\}[D_2]\{q\} \\ \mathrm{K} &= [D_3]\{q\}\end{aligned} \tag{35}$$

where

$$[N] = [S][A]^{-1},\ [D_1] = [B_1][S][A]^{-1}$$
$$[D_2] = [B_2][S][A]^{-1},\ [D_3] = [B_3][S][A]^{-1}$$

In the process of solution, it is required to evaluate the strain increment $\Delta\epsilon$. From Eq. (35), the strain increment is related to the displacements and the displacement increments by

$$\Delta\epsilon = \Delta\epsilon_0 + \zeta\Delta\mathrm{K} \tag{36}$$

where

$$\begin{aligned}\Delta\epsilon_0 &= [D_1]\{\Delta q\} + [q]\{D_2\}[D_2]\{\Delta q\} \\ \Delta\mathrm{K} &= [D_3]\{\Delta q\}\end{aligned}$$

Equations of Dynamic Equilibrium

Introducing the stress resultants for the cross section

$$L = \iint_s \sigma ds,\ M = \iint_s \sigma\zeta ds \tag{37}$$

where the integrations being taken over the cross section of the beam element, and substituting Eqs. (34), (35), and (37), into the Principle of Virtual Displacements equation, Eq. (15), one obtains

$$\sum_{n=1}^{n} [\delta q^*]([m]\{\ddot{q}^*\} + \{p\} + [h]\{q^*\} - \{Q\}) = 0 \tag{38}$$

where

$$\begin{aligned}[m] &= [J]^T \int_0^{\eta_{i+1}} [N]^T \begin{bmatrix}\tilde{m} & 0 & 0\\ 0 & \tilde{m} & 0\\ 0 & 0 & I\end{bmatrix} [N]d\eta[J] \\ \{p\} &= [J]^T \int_0^{\eta_{i+1}} (\{D_1\}L + \{D_3\}M)d\eta \\ [h] &= [J]^T \int_0^{\eta_{i+1}} \{D_2\}[D_2]Ld\eta[J] \\ \{Q\} &= [J]^T \int_0^{\eta_{i+1}} \tilde{m}[N]^T\{f\}d\eta\end{aligned} \tag{38a}$$

and $\tilde{m}$ is the mass per unit original length of the beam element, and I is the moment of inertia of the cross section. The integrations along the length of the beam element which appear in $\{p\}$ and $[h]$ may be performed numerically, for example, using the Gaussian quadrature scheme.[21] The axial force L and moment M at those integration stations will be described and evaluated later.

Stress-Strain Relations

Because of nonlinear material behavior, although the strain variation through the beam thickness, by the Bernoulli-Euler hypothesis, is linear, the variation of stress across the thickness is nonlinear. For computational convenience, the stresses are evaluated at selected Gaussian points across the thickness and the corresponding weighting function is used in evaluating the pertinent integrals by Gaussian quadrature. The strain-hardening behavior of the material may be accounted for by representing the material at each Gaussian station as consisting of equally-strained sublayers of elastic, perfectly plastic material, with each sublayer having the same elastic modulus but an appropriately different yield stress; this is the well-known mechanical sublayer model.[12,22,23]

An illustration of the method of computing the stress is presented as follows. One begins by knowing the sublayer stress $\sigma_{jk,i-1}$ at time t_{i-1} for the kth sublayer of the jth Gaussian station (layer), and the layer strain increment $\Delta\epsilon_{j,i}$ at time t_i (that is, the strain increment from time t_{i-1} to time

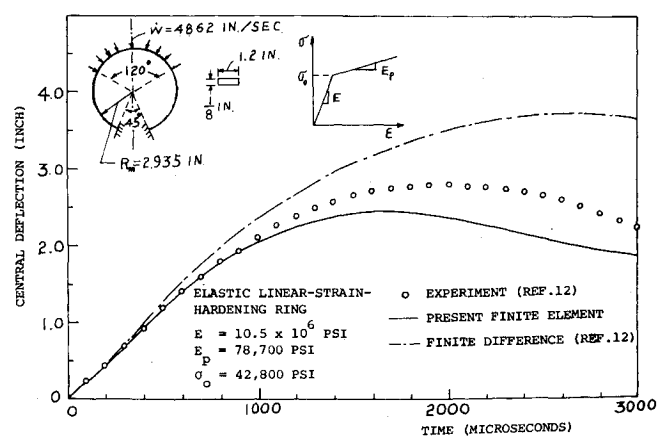

Fig. 3 Central deflection response for explosively-loaded 6061-T6 clamped circular ring.

t_i). One then takes a trial value (superscript t) of $\sigma_{jk,i}$ which is computed by assuming an elastic path:

$$\sigma_{jk,i}{}^t = \sigma_{jk,i-1} + E\Delta\epsilon_{j,i} \tag{39}$$

A check is then performed to see what the correct value of $\sigma_{jk,i}$ must be:

$$\begin{aligned} &\text{If } -\sigma_{ok} \leq \sigma_{jk,i}{}^t \leq \sigma_{ok} \text{ then } \sigma_{jk,i} = \sigma_{jk,i}{}^t \\ &\text{If } \quad \sigma_{jk,i}{}^t < -\sigma_{ok} \text{ then } \sigma_{jk,i} = -\sigma_{ok} \\ &\text{If } \quad \sigma_{jk,i}{}^t > \sigma_{ok} \text{ then } \sigma_{jk,i} = \sigma_{ok} \end{aligned} \tag{40}$$

where E is Young's modulus and σ_{ok} is the yield stress of the idealized elastic, perfectly plastic kth sublayer.

This procedure is applied to all sublayers of each layer or Gaussian station j; having done this, the axial force and moment can be determined by

$$\begin{aligned} L &= b\frac{h}{2}\sum_j\left(\sum_k \sigma_{jk}A_{jk}\right) \\ M &= b\frac{h}{2}\sum_j \zeta_j\left(\sum_k \sigma_{jk}A_{jk}\right) \end{aligned} \tag{41}$$

where b is the width and h is the thickness of the beam and A_{jk} is the mechanical sublayer weighting factor which is defined by

$$A_{jk} = (W_j/E)(E_k - E_{k+1}) \tag{42}$$

In Eq. (42) W_j is the Gaussian weighting factor and

$$E_k = (\sigma_k - \sigma_{k-1})/(\epsilon_k - \epsilon_{k-1}) \tag{43}$$

is the kth slope of the polygonal approximate stress-strain diagram. It can be verified that the relations $\Sigma_k A_{jk}/W_j = 1$, and $W_j\sigma_j = \Sigma_k A_{jk}\sigma_{jk}$ are satisfied.

If desired, the sublayer yield stresses may be treated as strain-rate dependent as described, for example, in Ref. 4.

Solution Method

The timewise central-difference scheme is used to solve the dynamic equations of equilibrium. In this scheme, the relations between displacements and displacement increments at any instant of time $t = t_i$ are

$$\{\Delta q^*\}_{t_i} = \{q^*\}_{t_i} - \{q^*\}_{t_{i-1}} \tag{44}$$

and

$$\{q^*\}_{t_i} = \{q^*\}_{t_0} + \{\Delta q^*\}_{t_1} + \{\Delta q^*\}_{t_2} + \ldots + \{\Delta q^*\}_{t_i}$$

At time t_i, the acceleration may be expressed in terms of displacement increments by the following central-difference finite difference expression:

$$\{\ddot{q}^*\}_{t_i} = [\{\Delta q^*\}_{t_{i+1}} - \{\Delta q^*\}_{t_i}]/(\Delta t)^2 \tag{45}$$

Employing Eq. (45), the dynamic equations of equilibrium (from Eq. (38)) at any time instant t_i becomes

$$\{\Delta q^*\}_{t_{i+1}} = \{\Delta q^*\}_{t_i} + (\Delta t)^2[M^*]^{-1}(\{F\} - \{P\} - [H]\{q^*\})_{t_i} \tag{46}$$

With the specified initial velocity $\{\dot{q}^*\}_{t_0}$ and the load acting at time zero, $\{F\}_{t_0}$, the calculation scheme commences by assuming the initial stress distribution is zero, and the increment of displacement between time-step zero and time-step one is

$$\{\Delta q^*\}_{t_1} = \{\dot{q}^*\}_{t_0}(\Delta t) + (\Delta t)^2[M^*]^{-1}\{F\}_{t_0} \tag{47}$$

After the calculation of $\{\Delta q^*\}_{t_1}$, the strain increment at any station or point in the element can be obtained from Eq. (36). With the strain increment available, the stress increment and stress is computed from the stress-strain relation. Then the stress resultants (i.e., the axial force and moment) are obtained from Eq. (41). Equation (46) furnishes the displacement increment for the next time step. The process is cyclic thereafter.

In order to insure the stability of the timewise numerical-integration method, the time-step size, Δt, must be small enough; for the problem of the present type, use is made of the criteria[24] defined by the linear problem as a guide for the initial selection of Δt values. Numerical experimentation then subsequently can provide the proper Δt to insure stability.

Other time integration schemes such as those discussed, for example, in Ref. 25 could be employed, if desired, to enable one to use larger time increments Δt.

Results and Discussion

A computer program employing this beam element has been developed, and numerical examples have been carried out. The first example problem discussed here is an elastic perfectly plastic clamped beam loaded impulsively over a spanwise segment centered at its midspan. Since there is symmetry with respect to both geometry and loading, only one-half span is modeled in the finite-element analysis with symmetry imposed at midspan. Figure 2 shows the present finite-element prediction for the midspan lateral displacement history vs both a finite-difference solution[12] and experimental results.[12] Very good agreement among these results is observed. The half-span was modeled with 30 finite-difference stations and with 10 finite elements, and the time-step sizes are $\frac{2}{3}$ μsec and 1 μsec for the finite-difference and the finite-element calculation, respectively. The 6061-T6 aluminum beam material was modeled as being rate-independent elastic, perfectly plastic for both calculations.

For this clamped beam problem, the use of formulation Eq. (22a) has been tested by the same timewise central-difference scheme and the same finite-element breakdown. The calculation was found to be numerically unstable for a time-step size as small as 0.1 μsec.

The second problem discussed is an explosively loaded clamped circular 6061-T6 ring. Figure 3 shows the deformation response history of the experimentally measured central radial (or vertical) deflection compared with finite-difference and the present finite-element predictions; the material is modeled as rate-independent, elastic, linear-strain hardening. Comparing these calculations with experiment, a somewhat stiffer response is predicted by the finite-element method: the peak deformation response is 12% less and it occurs 300 μsec before that observed experimentally, whereas the finite-difference prediction vastly overestimates the response. Again advantage was taken of symmetry by modeling half of the ring by 31 finite-difference stations or by 19 finite elements. The time-step size is 1 μsec in both numerical calculations.

To assess further the accuracy of the deformation profile predictions, experiment, the finite-difference, and the finite-element predicted deformation profiles are compared in Fig. 4 at 780 μsec and at 2880 μsec. At 780 μsec, both predictions are in reasonably close agreement with experiment, with the finite-element result being somewhat better. At 2880 μsec, the finite-element result exhibits somewhat "stiffer behavior" but the finite-difference prediction vastly overestimates the deformation. The reasons for these prediction discrepancies have not yet been firmly established. Incidentally, as illustrated in Ref. 12, the inclusion of a fairly weak dependence of the yield stress upon strain rate produces a significantly reduced response.

Finally, it is of interest to note that the matrices $\{p\}$ and $[h]$ given by Eq. (38a) are evaluated at each instant of time by employing Gaussian quadrature; in the present examples, 3 spanwise Gaussian stations and 4 depthwise Gaussian stations at each spanwise Gaussian station were employed.

The present finite-element formulation represented by Eq. (22) provides a significant improvement over the former conventional formulation, Eq. (22a), for analyzing the large, elastic-plastic transient deformations of structures. Application of the present formulation to complex shell structures will be of interest.

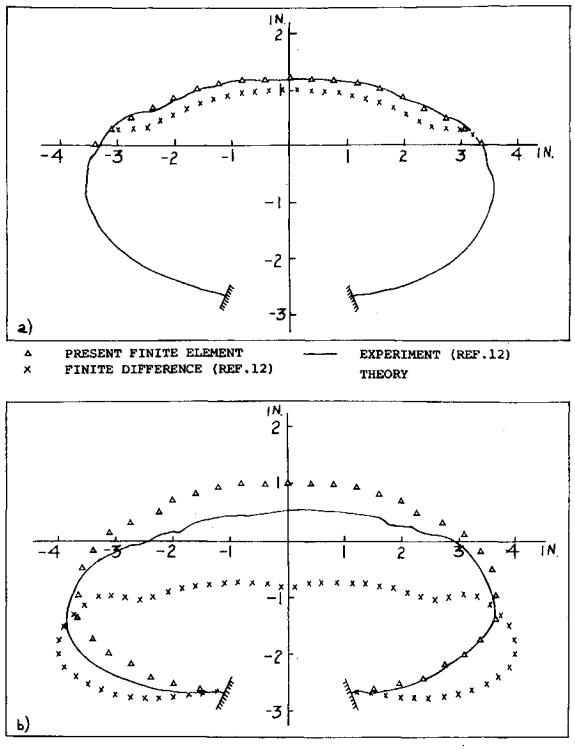

Fig. 4 Deformation profiles for explosively-loaded 6061-T6 clamped circular ring, a) experiment at 785 microseconds, theory at 780 microseconds; and b) experiment at 2854 -sec, theory at 2880 μsec.

References

[1] Pian, T. H. H. and Tong, P., "Basis of Finite Element Methods for Solid Continua," *International Journal for Numerical Methods in Engineering*, Vol. 1, 1969, pp. 3–28.

[2] Budiansky, B. and Radkowski, P. P., "Numerical Analysis of Unsymmetrical Bending of Shells of Revolution," *AIAA Journal*, Vol. 1, No. 8, Aug. 1963, pp. 1833–1842.

[3] Witmer, E. A., Balmer, H. A., Leech, J. W., and Pian, T. H. H., "Large Dynamic Deformations of Beams, Rings, Plates, and Shells," *AIAA Journal*, Vol. 1, No. 8, Aug. 1963, pp. 1848–1857.

[4] Morino, L., Leech, J. W., and Witmer, E. A., "PETROS 2: A New Finite Difference Method and Program for the Calculation of Large Elastic-Plastic Dynamically-Induced Deformations of General Thin Shells," BRL CR 12 (MIT-ASRL TR 152-1), Dec. 1969, U.S. Army Ballistic Research Lab., Aberdeen, Md.

[5] Kalnins, A., "Static, Free Vibration, and Stability Analysis of Thin Elastic Shells of Revolution," Rept. AFFDL-TR-68-144, March 1969, Air Force Flight Dynamics Lab., Wright-Patterson Air Force Base, Ohio.

[6] Cohen, G. A., "Computer Analysis of Asymmetrical Buckling of Ring-Stiffened Orthotropic Shells of Revolution," *AIAA Journal*, Vol. 6, No. 1, Jan. 1968, pp. 141–149.

[7] Svalbonas, V. and Agrisano, N., "Numerical Analysis of Shells—Vol. II: User's Manual for STARS II—Shell Theory Automated for Rotational Structures," Rept. FSR-AD2-01-68.5, Aug. 1968, Grumman Aircraft Engineering Corp., Bethpage, N.Y.

[8] Melosh, R. J., Diether, P. A., and Brennan, M., "Structural Analysis and Matrix Interpretive System (SAMIS)—Program Report," TN 33-307, Dec. 1966, Jet Propulsion Lab., Pasadena, Calif.

[9] MacNeal, R. H., ed., "The NASTRAN Theoretical Manual"; also McCormick, C., ed., "The NASTRAN User's Manual," Aug. 1969, NASA.

[10] Kotanchik, J. J., Yeghiayan, R. P., Witmer, E. A., and Berg, B. A., "The Transient Linear Elastic Response Analysis of Complex Thin Shells of Revolution Subjected to Arbitrary External Loading, by the Finite-Element Program SABOR5-DRASTIC," TR 70-206 (MIT-ASRL TR 146-10), April 1970, SAMSO, Air Force Space and Missile Systems Organization, Norton Air Force Base, Calif.

[11] Kotanchik, J. J. and Berg, B. A., "STACUSS 1: A Discrete-Element Program for the Static Analysis of Single-Layer Curved Stiffened Shells Subjected to Mechanical and Thermal Loads," SAMSO, Air Force Space and Missile Systems Organization, Norton Air Force Base, Calif. TR 70-125 (MIT-ASRL TR 146-9), Dec. 1969.

[12] Balmer, H. A. and Witmer, E. A., "Theoretical-Experimental Correlation of Large Dynamic and Permanent Deformations of Impulsively-Loaded Simple Structures," FDL-TDR-64-108 (MIT-ASRL TR 110-2), July 1964, Air Force Flight Dynamics Lab., Wright-Patterson Air Force Base, Ohio.

[13] Atluri, S., Witmer, E. A., Leech, J. W., and Morino, L., "PETROS 3: A Finite-Difference Method and Program for the Calculation of Large Elastic-Plastic Dynamically-Induced Deformation of Multilayer Variable-Thickness Shells," MIT-ASRL TR 152-2, Aug. 1970, MIT, Cambridge, Mass.

[14] Silsby, W., Sobel, L. H., and Wrenn, B. G., "Nonsymmetrical and Nonlinear Dynamic Response of Thin Shells, Vol. 1, User's Manual for STAR (Shell Transient Asymmetric Response)," LMSC B-70-68-19, Dec. 1968, Lockheed Missile & Space Co., Palo Alto, Calif.

[15] Stricklin, J. A., Martinez, J. E., Tillerson, J. R., Hong, J. H., and Haisler, W. E., "Nonlinear Dynamic Analysis of Shells of Revolution by the Matrix Displacement Method," Rept. 69-77, Feb. 1970, Aerospace Engineering Dept., Texas A & M Univ., College Station, Texas.

[16] Armen, H., Jr., Levine, H. S., and Pifko, A. "Elastic-Plastic Behavior of Plates Under Combined Bending and Stretching," AIAA, New York, 1970, pp. 224–238.

[17] Marcal, P. V., "Finite Element Analysis of Combined Problems of Nonlinear Material and Geometric Behavior," Rept. N00014-0007/1, March 1969, Div. of Engineering, Brown Univ., Providence, R.I.

[18] Hibbitt, H. D., Marcal, P. V., and Rice, J. R., "A Finite Element Formulation for Problems of Large Strain and Large Displacement," Rept. N00014-0007/2, June 1969, Div. of Engineering, Brown Univ., Providence, R.I.

[19] Salus, W. L., Ip, C., and VanDerlinden, J. W., "Design Considerations of Elastic-Plastic Structures Subjected to Dynamic Loads," *AIAA/ASME 11th Structures, Structural Dynamics, and Materials Conference*, AIAA, New York, 1970, pp. 145–153.

[20] Cantin, G. and Clough, R. W., "A Curved Cylindrical Shell Finite Element," *AIAA Journal*, Vol. 6, No. 6, June 1968, pp. 1057–1062.

[21] Kopal, Z., *Numerical Analysis*, Chapman and Hall Ltd., London 1961, p. 562.

[22] White, G. N., Jr., "Application of the Theory of Perfectly Plastic Solids to Stress Analysis of Strain Hardening Solids," Tech. Rept. 51, August 1950, Graduate Div. of Applied Mathematics, Brown Univ., Providence, R.I.

[23] Besseling, J. F., "A Theory of Plastic Flow for Anisotropic Hardening in Plastic Deformation of an Initially Isotropic Material," Rept. S.410, 1953 National Aeronautical Research Inst., Amsterdam, The Netherlands.

[24] Leech, J. W., Hsu, P. T., and Mack, E. W., "Stability of a Finite-Difference Method for Solving Matrix Equations," *AIAA Journal*, Vol. 3, No. 11, Nov. 1965, pp. 2173–2174.

[25] Nickell, R. E., "On the Stability of Approximation Operators in Problems of Structural Dynamics," MM 69-4116-14, 1969, Bell Telephone Labs., Whippany, N.J.